Cryosol Synthesis of Nanocrystalline Alumina

A. I. Mamchik, S. V. Kalinin, and A. A. Vertegel*

Inorganic Chemistry Division, Department of Chemistry, Moscow State University, Vorobyovy Hills, 119899, Moscow, Russia

Received May 1, 1998. Revised Manuscript Received July 27, 1998

In the present research we employed the newly developed cryosol technique for the preparation of nanocrystalline $Al(OH)_3$. The technique yields sols of aluminum hydroxide stable under a wide range of pH values and concentrations. Freeze-drying of the sols results in the formation of aluminum hydroxide powders with extremely low density and small particle size. Thermal behavior and phase evolution of the cryosol-derived aluminum hydroxide has been studied. According to X-ray diffraction data, annealing of cryosol-derived aluminum hydroxide results in amorphous alumina stable up to 800 °C. However DTA, electron diffraction, and ^{27}Al NMR studies indicate that the samples amorphous to X-ray diffraction are composed of crystalline nanoparticles. The thermal stability of nanocrystals is supposed to be due to the high uniformity of the particles size distribution, the latter resulting from the synthetic method employed.

Introduction

Nowadays aluminum oxide powders are widely used in various solid-state materials such as adsorbents and catalysts. One of the main methods for preparation of these materials is thermal decomposition of aluminum hydroxides. Depending on the conditions of precipitation and further decomposition, various mechanisms of dehydration can be observed[1−5] (Figure 1).

The reaction path of the system during heating is primarily governed by the phase composition and morphology of initial aluminum hydroxide particles. The latter also influences the microstructural properties (average grain size, porosity, etc.) of the resulting material. Therefore, physicochemical properties of Al_2O_3-based materials are strongly affected by the synthetic method employed for the preparation of initial aluminum hydroxide.

The main techniques for preparation of $Al(OH)_3$ can be subdivided into three basic groups: (a) rapid precipitation from aqueous solution containing either cationic $[Al(H_2O)_6^{3+}]$ or anionic ($[Al(OH)_6]^{3-}$) complexes of aluminum;[6] (b) slow hydrolysis of aluminum salts in the presence of urea or other basic agent (method of nascent reagent)[2]; and (c) hydrolysis of aluminum alkoxides.[7]

Recently a novel cryosol technique has been developed for the preparation of oxide ceramics. The method is based on the treatment of aqueous solution of multivalent metal nitrate by anion-exchange resin in the OH-form with subsequent freeze-drying of metal hydroxide sols obtained[8] (Figure 2). Previously[9,10] we reported the cryosol synthesis and properties of amorphous aluminum hydroxide. In the present research an attempt was made to investigate the sequence of phase transformations during thermal decomposition of cryosol-derived aluminum hydroxide.

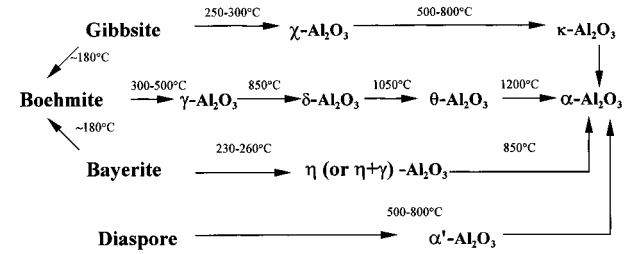

Figure 1. Transformations of aluminum oxides.

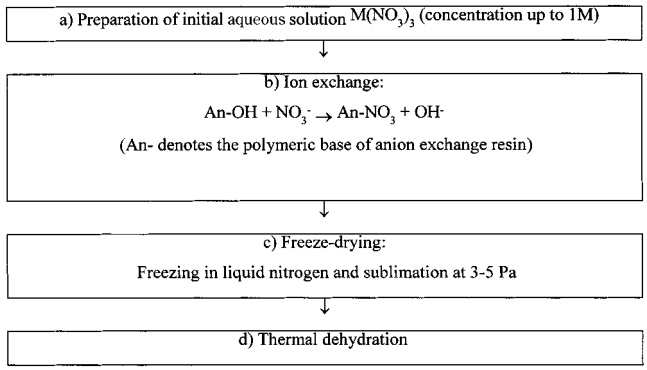

Figure 2. The scheme of the cryosol technique.

* Corresponding author. E-mail: al@inorg.chem.msu.ru.

(1) Toropov, N. A.; Barzakovsky, V. P.; Bondar, I. A.; Udalov, Yu. P. *Phase diagrams of silicate systems;* Nouka: Leningrad; 1969.
(2) Wefers, K.; Misra, C. *Oxides and Hydroxides of Aluminum*; Alcoa Laboratories: Pittsburgh, 1987; p 92.
(3) Pyzalski, M.; Wojcik, M. *J. Therm. An.* **1990**, *36*, 2147.
(4) Novak, C.; Pokol, G.; Izvekov, V.; Gal,T. *J. Therm. An.* **1990**, *36*, 1895.
(5) Carim, A. H.; Rohrer, G. S.; Dando, N. R.; Rohrer, C. L.; Tzeng, S.-Y.; Perrotta, A. J. *J. Am. Ceram. Soc.* **1997**, *80*, 2677.
(6) Krivorutchko, O. P.; Fedotov, M. A.; Buyanov, P. A. *Russ. J. Inorg. Chem.* **1978**, *23* (9), 2242.
(7) Tsai, M. T.; Shih, H. C. *J. Mater. Sci. Lett.*, **1993**, *12*, 1025.
(8) Vertegel, A. A.; Kalinin, S. V.; Oleynikov, N. N.; Tretyakov, Yu. D. *J. Non-Cryst. Solids* **1995**, *181*, 146.
(9) Vertegel, A. A.; Tomashevich, K. V.; Oleynikov, N. N.; Kheifets, L. I. *Inorg. Mater.* **1995**, *31* (4), 457.
(10) Mamchik, A. I.; Vertegel, A. A.; Tomashevich, K. V.; Oleynikov, N. N.; Ketsko, V. A.; Tretyakov, Yu. D. *Russ. J. Inorg. Chem.*, **1998**, *43* (1), 18.

10.1021/cm9803206 CCC: $15.00
Published on Web 10/29/1998

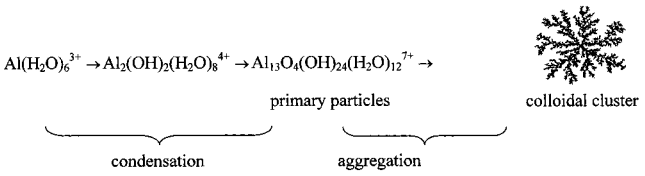

Figure 3. Mechanism of the formation of colloidal aggregates.

Table 1. pH Values and Compositions of Colloid Solutions Prepared by Anion-Exchange Treatment

samples	pH	*x*	formulas
A1	3.48	0.42	$Al(OH)_{0.42}(NO_3)_{2.58}$
A2	3.60	1.62	$Al(OH)_{1.62}(NO_3)_{1.38}$
A3	3.78	2.46	$Al(OH)_{2.46}(NO_3)_{0.54}$
A4	5.72	2.92	$Al(OH)_{2.92}(NO_3)_{0.08}$
A5	6.15	2.95	$Al(OH)_{2.95}(NO_3)_{0.05}$
A6	6.78	2.98	$Al(OH)_{2.98}(NO_3)_{0.02}$
A7	7.00	3.0	$Al(OH)_3$

Table 2. pH Values and Compositions of the Solutions Obtained by Hydrolysis in the Presence of NH_4OH.

samples	x	formulas
N1	0.76	$Al(OH)_{0.76}(NO_3)_{2.24}$
N2	1.24	$Al(OH)_{1.24}(NO_3)_{1.76}$
N3	1.58	$Al(OH)_{1.58}(NO_3)_{1.42}$
N4	2.43	$Al(OH)_{2.43}(NO_3)_{0.57}$
N5	2.59	$Al(OH)_{2.59}(NO_3)_{0.41}$
N6	3.00	$Al(OH)_3$

Experimental Section

The initial 0.1 M solutions of aluminum nitrate were prepared from solid $Al(NO_3)_3 \cdot 9H_2O$ (reagent grade) and distilled water. The solutions were repeatedly treated by small (≈1 g) portions of anion-exchanger IRA-410 (Amberlite). The ion-exchanger was preliminary transferred into the OH−form by 1 M KOH and washed to pH = 7 with distilled water. After each cycle of the treatment, the ion-exchange resin was separated and the solutions were aged for ∼30 min in order to achieve the hydrolytic equilibrium as determined by pH measurements on a ChemCadet (Cole-Parmer) instrument**.** Ion exchange results in subsequent formation of di-, oligo-, and polymeric aluminum hydroxocomplexes (Figure 3). Contrary to conventional hydrolysis, anion exchange treatment yields aluminum hydroxide sols stable under a the wide range of pH values ($4 < pH < 7$) and concentrations. In the present research, we studied colloid solutions with an aluminum concentration of 0.1 M with different pH values. pH values and composition of the samples synthesized by the anion exchange method are listed in Table 1.

To compare the evolution of aluminum species in solution during anion-exchange treatment with that during conventional hydrolysis, the solutions of aluminum hydroxynitrates $Al(OH)_x(NO_3)_{3-x}$ ($0 < x < 2.6$) were prepared by the reaction of a calculated amount of 1 M $Al(NO_3)_3$ aqueous solutions and concentrated NH_4OH with further dilution. The resulting concentrations of aluminum were 0.1 M. The solutions were aged for 2 weeks to ensure the achievement of hydrolytic equilibrium. The degree of hydrolysis, *x*, was determined by pH-metric titration on a ChemCadet (Cole-Parmer) instrument. Here we studied solutions of $Al(OH)_x(NO_3)_{3-x}$ with the compositions given in Table 2.

The addition of NH_4OH beyond $x > 2.6$ leads to spontaneous precipitation. However, we prepared an inhomogeneous sample, N6 ($x = 3.0$), in order to compare its properties with those of anion-exchange-derived sols.

The samples A4−A6, with higher degrees of hydrolysis and composition close to $Al(OH)_3$, were frozen in liquid nitrogen (block freezing). The white icy granules that result from the rapid freezing were then dried in a commercial laboratory freeze-dryer SMH 15 (USIFROID). The pressure during the process was sustained at 3−5 Pa. The temperature of the heating plate was gradually increased from −65 °C to 50 °C for 24 h. After completion of the freeze-drying step, the resulting hydroxide precursors were stored in a desiccator.

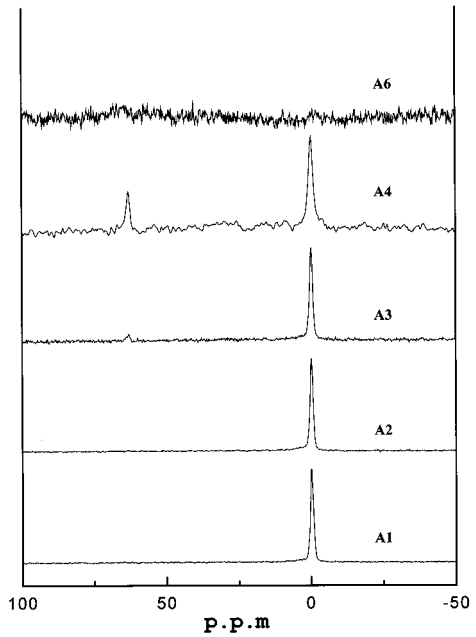

Figure 4. ^{27}A1 NMR spectra of samples A1−A4 and A6.

Thermogravimetric (TG) and differential thermal analyses (DTA) of the freeze-dried samples were performed on Ulvac thermobalances (Sinku-Riko). The heating rate was chosen to be 10 K/min. The samples were also characterized by scanning (SEM) and transmission (TEM) electron microscopy as well as by electron diffraction on a JEM FX2000II electron microscope (JEOL). X-ray diffraction spectra (XRD) were taken on a DRON-2 conventional diffractometer (Co Kα radiation).

^{27}Al NMR spectra for solutions and solids were obtained at 78.205 MHz on an MSL-300 (Bruker) spectrometer. All measurements were made at room temperature. Spectra were recorded after applying an excitation pulse of 15° (2 μs) with an accumulation interval of 1s between successive accumulations to avoid cumulative effects. A 1 M aqueous solution of $[Al(H_2O)_6]^{3+}$ was used as the external standard in all cases. The total number of accumulations was varied from 1000 to 6000 impulses per sample.

Results

The solutions of aluminum hydroxynitrates and aluminum hydroxide sols prepared by anion exchange were studied by ^{27}Al NMR (Figure 4). The spectra obtained for different degrees of hydrolysis, *x*, are similar to those previously reported for hydroxynitrates prepared by traditional routes.[11−13] One should note the following main features of the spectra obtained. For the samples on the initial stages of anion-exchange treatment, only the peak at 0 ppm corresponding to octahedrally coordinated aluminum can be clearly seen.[11] The subsequent exchange of anions increases the degree of hydrolysis (*x*) and the peak at 62.5 ppm appears on the spectra for $x > 2$. This peak is usually ascribed to tetrahedrally coordinated aluminum in the Keggin-type cation[11] $Al_{13}O_4(OH)_{24}(H_2O)_{12}^{7+}$. However, anion-exchange enables one to obtain the NMR spectra for sols

(11) Fedotov, M. A.; Krivorutchko, O. P.; Buyanov, P. A. *Russ. J. Inorg. Chem.*, **1978**, *23* (9), 2326.
(12) Akitt, J. W.; Greenwood, N. N.; Khandelwal, B. L.; Lester,G. D. *J. Chem. Soc., Dalton. Trans.* **1972**, *5*, 604.
(13) Akitt, J. W.; Farthing, A. *J. Magn. Res.* **1978**, *32*, 345.

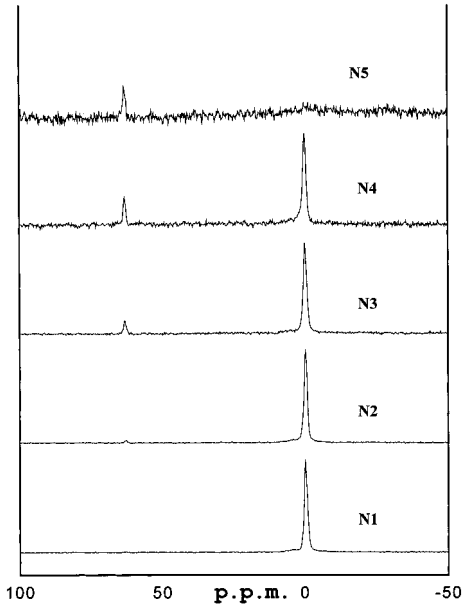

Figure 5. ^{27}A1 NMR spectra of samples N1−N5.

with higher degrees of hydrolysis ($x > 2.5$) that cannot be prepared by conventional hydrolysis. These spectra are characterized by a high level of noise that is due to the low mobility of aluminum in polymeric hydroxo-complexes. ^{27}Al NMR spectra for the reference solutions N1−N6 prepared by conventional hydrolysis correspond well to the previously reported data[11−13] (see Figure 5).

The freeze-drying of the sols results in white, very friable, nonhygroscopic powders ($\rho \sim 0.05$ g/cm^3). The as-prepared samples are amorphous to X-ray and electron diffraction. SEM micrographs of the as-prepared sample A6 are shown in Figure 6. One can see that the sample is made up of very thin platelets that are transparent to the electron beam. Such two-dimensional structures are characteristic for the block-frozen samples obtained by the freeze-drying technique. The explanation of this effect is that a large portion of a solution, due to the low thermoconductivity of water, solidifies layer-by-layer, being immersed into liquid nitrogen.[14]

The ^{27}Al NMR spectrum of the freeze-dried sample A6 (cryosol) is shown on Figure 7. Only one broad line is observed due to the strong dipole−dipole interaction in the solid phase. The spectrum can be fitted by one Lorentzian with a maximum at 26 ppm. However, the value of the chemical shift observed ($\delta = 26$ ppm) does not correspond to either octahedral or tetrahedral coordination of aluminum ($\delta_{\mathrm{Al(octahedral)}} = 0$ ppm and $\delta_{\mathrm{Al(tetrahedral)}} = 62.5$ ppm). This probably indicates the presence of aluminum both in octahedral and tetrahedral coordination. Indeed, fitting the spectrum by two Lorentzians results in broad peaks with chemical shifts at $\delta_1 = 4$ and $\delta_2 = 63$ ppm. These values are in good agreement with the chemical shifts expected for aluminum in tetrahedral and octahedral coordination.

^{27}Al NMR spectra of the freeze-dried samples N1−N6 (NH_4OH hydrolysis) are shown on Figure 8. For the samples N1, N2, and N3 ($x < 2.5$), the NMR spectra

(14) Tretyakov, Yu. D.; Oleynikov, N. N.; Shlyahtin, O. A. *Cryochemical Synthesis of Advanced Materials*; Chapman & Hall: London, 1997; p 323.

Figure 6. SEM micrographs of the sample A6: (a) ×3000 and (b) ×30000.

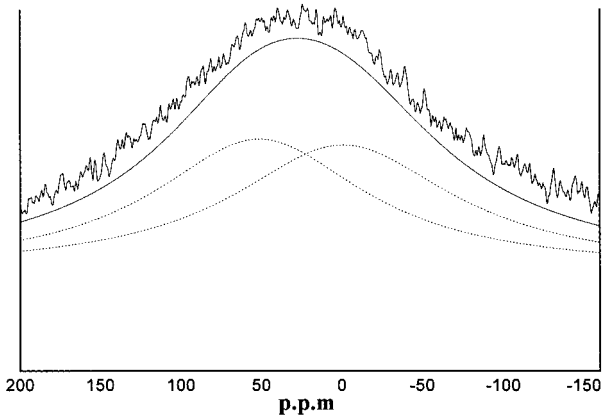

Figure 7. Solid-state ^{27}A1 NMR spectrum of the as-prepared cryosol-derived sample A6 (two-Lorentzian fit is shifted down).

cannot be fitted by one Lorentzian. Fitting by two Lorentzians results in two peaks with significantly different width (see Figure 9b). Both peaks are centered at $\delta_1 = 0$ ppm, thus suggesting the presence of aluminum in octahedral coordination. The relatively narrow peak (I) corresponds to aluminum with relatively high mobility (most likely in the form of $[Al(H_2O)_6]^{3+}$ captured in a hydroxide matrix), while the wide peak (II)

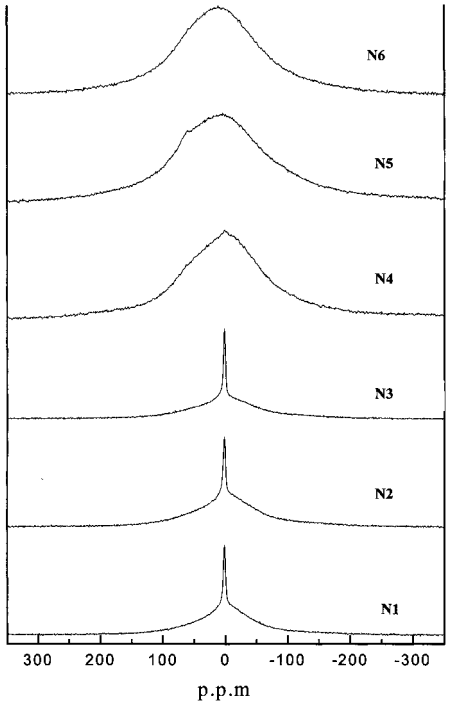

Figure 8. Solid-state ^{27}A1 NMR spectra of the freeze-dried samples N1−N6.

corresponds to aluminum in the solid phase with strong dipole−dipole interaction. With the following increase of x ($x \geq 2.5$), NMR spectra contain one broad asymmetric peak similar to that obtained for cryosol-derived sample. These peaks can be fitted by two Lorentzians with maximums at $\delta_1 = 3$ ppm and $\delta_2 = 60$ ppm, indicating the presence of both tetrahedrally and octahedrally coordinated aluminum (see Figure 9a).

Cryosol-derived samples A4-A6 were studied by thermal analysis. The weight loss observed was ca. 50%. This value is higher than that for crystalline samples of aluminum hydroxide. For instance, the weight loss during the thermal dehydration of gibbsite is ca. 35%,[2] which well-corresponds to the formula $Al(OH)_3$. Contrary to aluminum hydroxides prepared by traditional techniques, a well-defined exothermal effect appears on the DTA curves of the cryosol-derived samples in the temperature range 240−265 °C (see Figure 10). In hydroxide systems, such an effect can be ascribed only to crystallization of the samples. One can see that the temperature of the process slightly increases with the pH value of the initial sol. In our opinion, this effect is associated with the decrease of remaining amount of NO_3^- captured by the colloid particles in the course of anion exchange.

To determine the phase composition of the system after crystallization observed by DTA, the samples were annealed at 300 °C (1 h) and studied by means of X-ray diffraction analysis. However, XRD analysis showed that the samples did not contain any crystalline phase. Moreover, it was found that very broad diffraction peaks of γ-Al_2O_3 appeared on the XRD patterns only after annealing at 800 °C (Figure 11). At the same time, no thermal effect appears on the DTA curves at this temperature. Thus, crystallization is observed by DTA at less than 300 °C, while XRD analysis suggests crystallinity only after annealing at 800 °C.

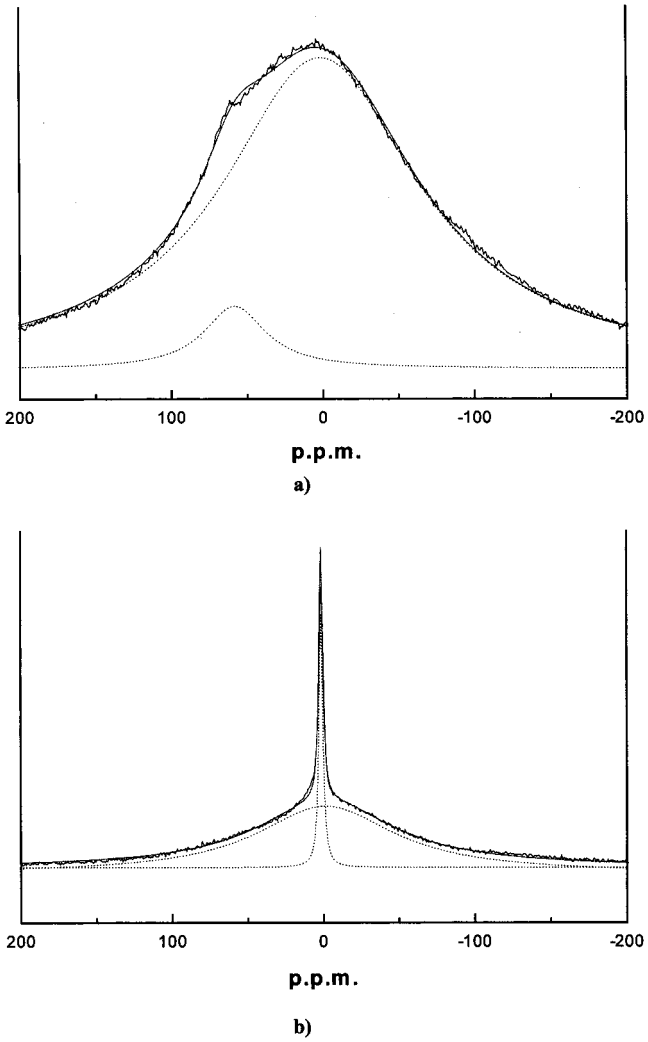

Figure 9. Two-Lorentzian fit of the NMR spectra shown in Fig. 8: (a) sample N5 and (b) sample N2.

To explain this observation, one should take into account that XRD analysis can be used for identification of a crystalline phase characterized by a grain size larger than 100−150 Å. At the same time, the colloid aggregates are made of primary particles with much smaller size [the diameter of the hydroxocomplexes (Al_{13}) that are believed to be the primary particles during formation of aluminum hydroxide[11] is about 18 Å]. Thus, one can suppose that the exothermal effect observed by DTA corresponds to crystallization within primary particles forming colloidal aggregates. After this, a sample remains amorphous to XRD analysis because of the very small size of the coherent scattering domain. The noticeable increase in grain size occurs only at elevated temperature due to the low density and high uniformity of the sample.

The suggested hypothesis was confirmed by electron diffraction measurements. Indeed, electron diffraction can be observed for the smaller crystallites sizes than X-ray diffraction ($d \geq 50$ Å). The TEM micrographs and ED patterns for the as-prepared sample A6 and the same sample annealed at $T = 500$ °C and 550 °C (1 h) are shown in Figure 12. The ED pattern is clearly seen in Figure 12c, indicating the presence of crystalline α-Al_2O_3 after annealing at 550 °C. At the same time, XRD analysis of this sample does not result in a

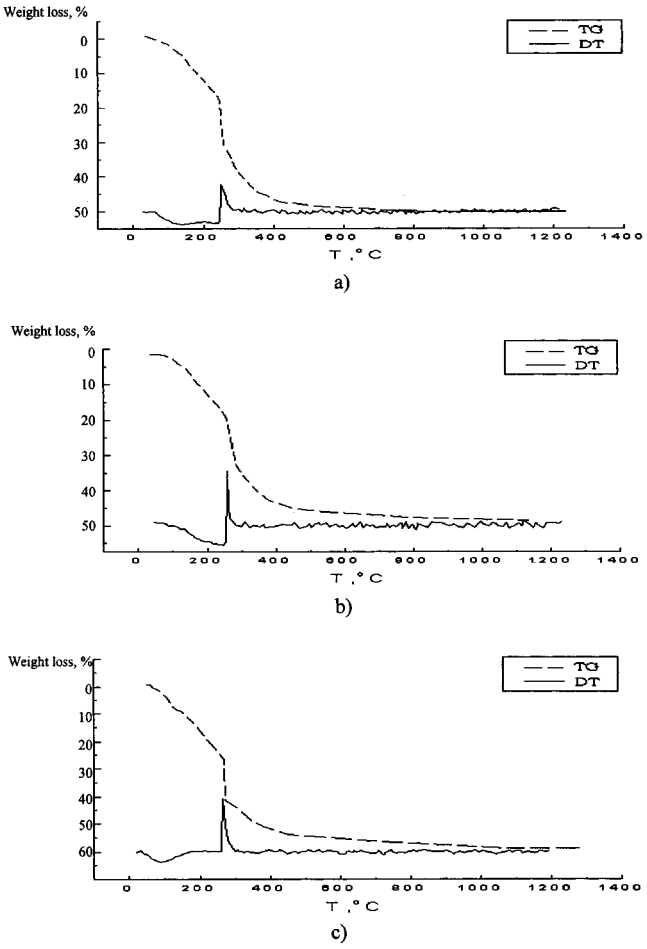

Figure 10. TG and DTA of the series "A" samples (the DTA signal is given in arbitrary units): (a) sample A4, (b) sample A5, and (c) sample A6.

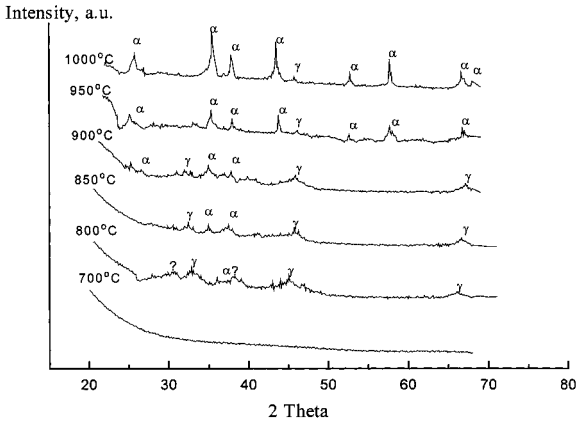

Figure 11. X-ray diffraction spectra of A6 sample during the thermal treatment.

diffraction pattern. Only three very broad lines can be seen in the ED pattern of the sample annealed at $T =$ 500 °C. As one can see from the Figure 12b, these reflections can also be attributed to α-Al_2O_3 rather than to γ-Al_2O_3. At the same time, broad lines seen on the ED pattern of the as-prepared sample cannot be attributed to any aluminum oxide or hydroxide.

The phase transition at ≈250 °C can be detected by means of the solid state ^{27}Al NMR studies. The NMR spectrum of the sample A6 annealed at 300 °C (1 h) is shown in Figure 13. Similarly to the spectrum of the as-prepared sample (Figure 7), the spectrum of the annealed sample contains a broad peak, indicating strong dipole−dipole interactions in the solid state. However, the maximum in Figure 7 can be resolved into two Lorenzians corresponding to aluminum in both octahedral and tetrahedral coordination. The NMR spectrum for the sample annealed at 300 °C can be fitted by one Lorentzian at $\delta = 0$ ppm, corresponding to aluminum in octahedral coordination. As one can see from Figure 13, the spectrum can also be fitted by two Lorentzians with maximums at $\delta_1 = 0$ ppm and $\delta_2 =$ 63 ppm. The second maximum may be attributed to aluminum in tetrahedral coordination; however, its amount is much less than in the case of the as-prepared sample. Thus, NMR data probably confirms the structural change between room temperature and 300 °C. It should be noted, that in α-alumina all aluminum atoms are octahedrally coordinated, while γ-alumina contains a significant amount (approximately one-third) of aluminum atoms in tetrahedral coordination. Thus, solid-state NMR data are in good agreement with ED measurements.

Discussion

The thermal stability of the nanocrystallites can be explained from the viewpoint of the theory suggested by Lifshits and Slezov.[15,16] According to LS, the solid-state system with the narrow particles' size distribution develops during thermal treatment sufficiently more slowly than that characterized by the broad size distribution. This is due to the fact that the driving force of the crystal growth is determined by the difference between chemical potentials of the largest and the smallest particles. Thus, the system with the broad size distribution easily undergoes recrystallization, while the uniform system tends to be relatively inert, even if it consists of the very small particles (see Figure 14).

In the case of the cryosol technique, the uniformity of the particles' size is predetermined by the method of the synthesis. Indeed, the ion exchange results in the formation of a restricted number of polymeric hydroxo-complexes with nanometric sizes (primary particles), which are assembled into colloidal aggregates by relatively weak bonds (see Figure 3). The freeze-drying fixes the structures prepared in a colloid solution and converts them into the solid state without significant change. Therefore, the solid-state system consisting of the uniform primary particles should be stable to heat.

Summarizing the ^{27}Al NMR, ED, and XRD data, the phase evolution of aluminum hydroxide synthesized by the cryosol technique may be represented by the following scheme:

$$\text{amorphous phase} \xrightarrow{\approx 250\ ^\circ\text{C}} \alpha\text{-}Al_2O_3 \xrightarrow{\approx 800\ ^\circ\text{C}} \gamma\text{-}Al_2O_3 \xrightarrow{\approx 950\ ^\circ\text{C}} \alpha\text{-}Al_2O_3$$

Such behavior can be understood from the viewpoint of the recent data[17] on the relative stability of nanocrys-

(15) Lifshits, I. M.; Slyosov, V. V. *ZETF* **1958**, *35*, 479.
(16) Lifshits, I. M.; Slyosov, V. V. *Solid State Phys.* **1959**, *1*, 1401.
(17) McHale, J. M.; Auroux, A.; Perrotta, A. J.; Navrotky, A. *Science* **1997**, *277*, 788.

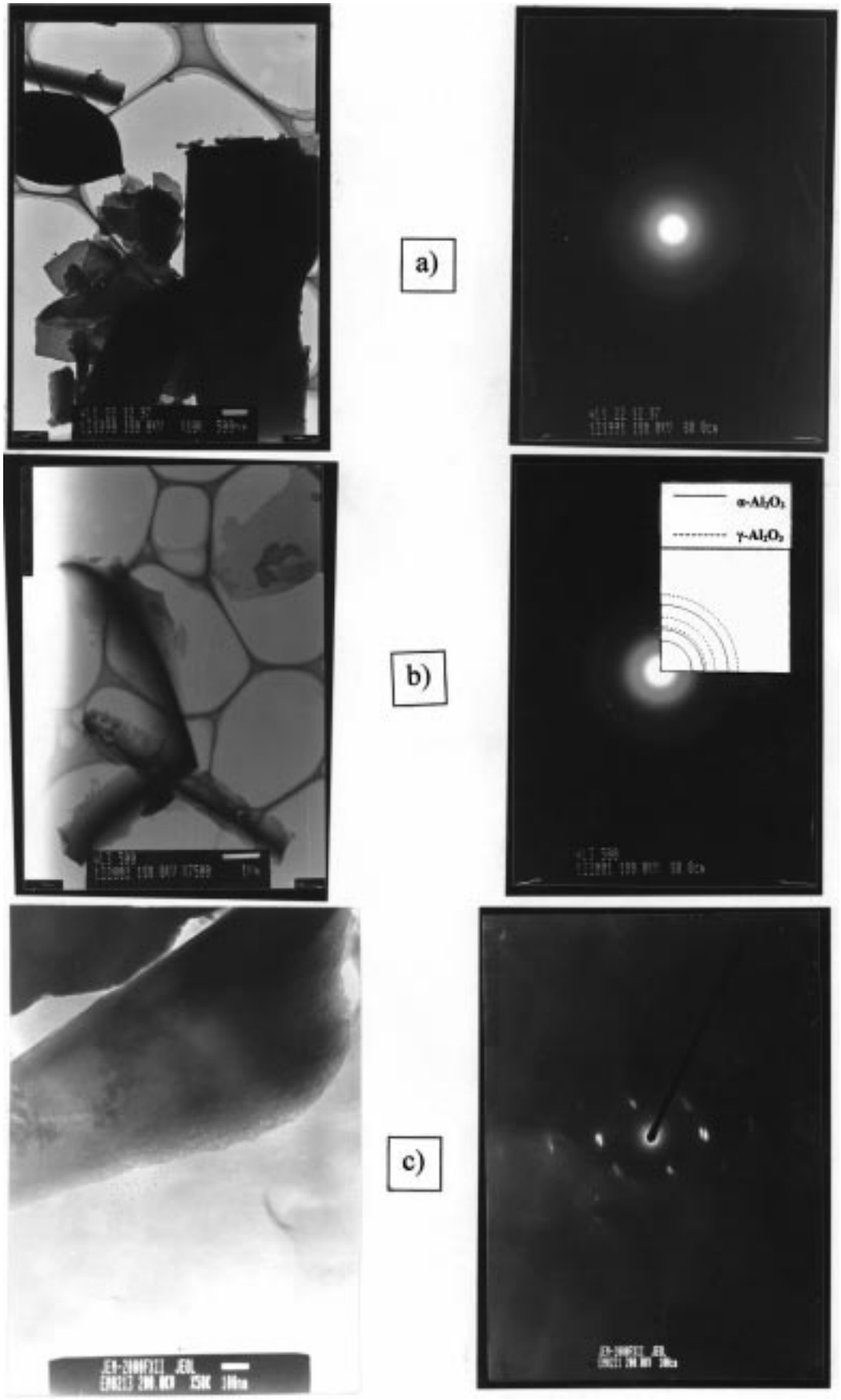

Figure 12. TEM and ED data of the sample A6: (a) as-prepared sample, (b) sample annealed at 500 °C, and (c) sample annealed at 550 °C.

talline α- and γ-aluminas. According to ref 17, γ-alumina becomes the thermodynamically stable phase when its particle size is less than ca. 5 nm, while α-alumina is more stable for the greater particle sizes.

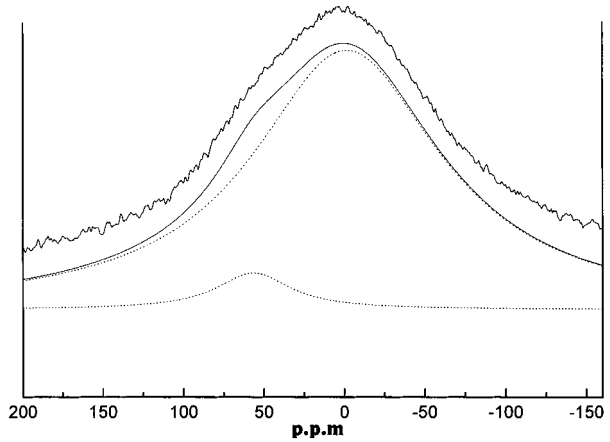

Figure 13. ^{27}Al solid-state NMR spectrum of the sample A6, annealed at 300 °C (two-Lorentzian fit is shifted down).

In our experiments, α-Al_2O_3 first appears under kinetically controlled conditions as a result of thermal decomposition of amorphous hydroxide. Thus obtained nanocrystalline α-Al_2O_3 is thermodynamically unstable and undergoes slow transition to the stable γ-alumina. However, this process is accompanied by the grain growth, and at a certain grain size α-alumina becomes the thermodynamically stable phase. Thus, γ-Al_2O_3 transforms back to α-Al_2O_3.

Conclusions

In the present work, we showed that the cryosol technique results in highly dispersed powders of aluminum oxides characterized by the wide temperature interval of stability of nanocrystalline phase. The crystallization is supposed to take place within primary particles forming colloidal aggregates. Thermal stability of nanocrystals is due to the high uniformity of the particles size distribution, the latter resulting from the synthetic method employed.

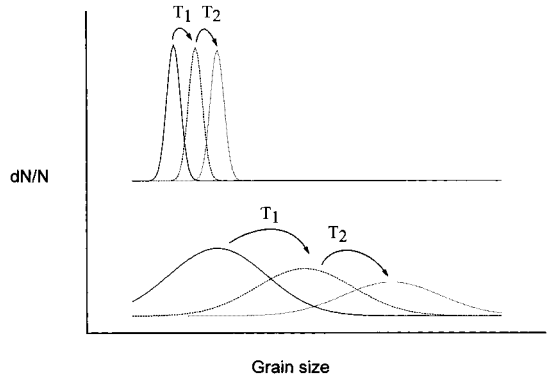

Figure 14. Schematic plot of the evolution of a solid-state system charaterized by narrow (a) and broad (b) particles size distribution during subsequent thermal treatments T_1 and T_2.

Acknowledgment. The paper was partially supported by the Russian Foundation for Basic Research (grant No. 96-03-33122a). We also grateful to Dr. V. I. Privalov (N. S. Kurnakov Institute for General and Inorganic Chemistry) for carrying out NMR measurements. A.I.M. and S.V.K. also express their deep gratitude to the International Soros Foundation (grants s97-345 and s97-1036).

CM9803206